Nanomed Res J 7(3):301-311, Summer 2022

RESEARCH ARTICLE

Impact of green-synthesized silver nanoparticles on cognitive function and fluorescence spectroscopy of redox status in the hippocampus

Sepideh Tarbali[1,2], Nasser Karimi[3], Mehran Alavi[3], Maryam Zahmatkesh[1,2,4*]

[1] Electrophysiology Research Center, Neuroscience Institute, Tehran, Iran, Tehran University of Medical Sciences, Tehran, Iran

[2] Department of Neurosciences and Addiction Studies, School of Advanced Technologies in Medicine, Tehran University of Medical Sciences, Tehran, Iran

[3] Nanobiotechnology Department, Faculty of Innovative Science and Technology, Razi University, Kermanshah, Iran

[4] Cognitive Sciences and Behavioral Research Center, Tehran University of Medical Sciences, Tehran, Iran

ARTICLE INFO

Article History:
Received 22 May 2022
Accepted 15 Jul 2022
Published 01 Aug 2022

Keywords:
Green-synthesized silver nanoparticles
Hippocampus
Redox status
Lipophilic fluorescent products

ABSTRACT

Silver nanoparticles exposure is inevitable due to their use in medical products and the food industry. They cross the blood–brain barrier and accumulate in the cerebrum and little information is available regarding their neurotoxicity. We investigated the potential alterations in hippocampal cognitive function and redox status after exposure to green-synthesized silver nanoparticles (AgNPs). The AgNPs was synthesized by Myrtle leaf extracts. After the stereotaxic surgery, the effects of different doses of intra-cerebroventricular-AgNPs administration were evaluated on spatial working memory, passive avoidance test, novel object recognition, and anxiety in male Wistar rats. The hippocampal malondialdehyde levels, and superoxide dismutase activity along with the lipophilic fluorescent products (LFPs) that are end products of lipid peroxidation were measured. The AgNPs had spherical, triangular, and hexagonal shapes with no aggregation. The average diameter size of AgNPs was 91.68 nm and the charge status was -17.4 mV. The AgNPs (1, 10, and 100 ppm) caused the memory impairment and induced anxiety-like behaviors. They raised the malondialdehyde and lowered the superoxide dismutase activity. Higher LFPs were identified in the hippocampus. Low dose of AgNPs (0.1 ppm) maintained hippocampal redox homeostasis and caused no cognitive decline. AgNPs (10 and 100 ppm) induced the high levels of LFPs, impaired memory, and altered the hippocampal redox homeostasis but the low dose (0.1 ppm) did not. Determining the pattern of variations in the spectrum of LFP fluorescent may introduce new indices for determining the nanoparticles toxicity and to make future safe classes of AgNPs in food and drug industries.

How to cite this article
Tarbali S., Karimi N., Alavi M., Zahmatkesh M. Impact of green-synthesized silver nanoparticles on cognitive function and fluorescence spectroscopy of redox status in the hippocampus. Nanomed Res J, 2022; 7(3): 301-311. DOI: 10.22034/nmrj.2022.03.010

INTRODUCTION

Frequent use of silver nanoparticles (AgNPs) in medical products generates potential risks for human health [1]. The orally administered nanoparticles cross the blood–brain barrier [2, 3] and little information is available regarding their interactions with the central nervous system macromolecules [4]. The nanoparticles show a tendency to accumulate in the brain [5]. Therefore, it is essential to investigate their neurotoxicity.

While several studies have demonstrated AgNPs toxicity on neuronal cells [6, 7], their anti-inflammatory and protective effects have also been reported [8, 9]. The noxiousness of AgNPs has been reported, but their hormesis effects have been overlooked [10]. Hormesis is a dose-dependent effect, as a low dose stimulates and a high dose inhibits certain targets [11].

Moreover, the cytotoxicity of AgNPs begins

* Corresponding Author Email: *zahmatkm@tums.ac.ir*

with the silver ions release [12] and induction of oxidative stress [13]. The green synthesis reduces the toxicity [9, 14] by stabilizing AgNPs [15, 16]. Myrtle (Myrtus communis L., Myrtaceae), a traditional medicine plant [17] could be used for AgNPs green synthesis [18, 19].

This study aimed to determine the possible cognitive alterations after intra-cerebroventricular (ICV) administration of different doses of green-synthesized silver nanoparticles (AgNPs). The working memory, passive avoidance test, novel object recognition, and the anxiety behavior were evaluated. Hippocampal redox status was evaluated via malondialdehyde (MDA) and superoxide dismutase (SOD) activity measurements. The reaction of aldehydes such as MDA with proteins or phospholipids produces lipophilic fluorescent products [20]. We have evaluated the hippocampus redox status by fluorescence spectroscopy of lipophilic fluorescent products (LFPs). The inherent fluorescence property is specific feature of LFPs which may change in different microenvironments [21]. Autofluorescence bioproducts are more sensitive than MDA[22] and a more reliable marker of tissue redox status.

MATERIAL AND METHODS

Chemicals

The $AgNO_3$ (CAS Number: 7761-88-8) was purchased from Sigma-Aldrich. For animal anesthesia, the Ketamine hydrochloride and Xylazine were purchased from Alfasan (Woerden, Holland). The hippocampal total protein, MDA, and SOD were measured by kit (TebPazhouhan Razi, Iran).

Synthesis of AgNPs with the M. communis plant

The plant was collected from the grid reference of 34.9805° N, 46.2720° E, from Bayangan Mountains in the west of Iran. After washing with the distilled water, 10 g of amassed leaves were air-dried to prepare the aqueous leaf extract. The dried leaves powder was boiled by 150 mL of deionized water at 60 ℃. After filtration, the suspension was stored at 4 ˚C till biochemical analysis [23].

The AgNPs was synthesized by adding 50 mL of $AgNO_3$ (0.001 M) to the 50 mL of leaf aqueous extract at 25 ℃ under stirred conditions for 48 h. Then, the solution was centrifuged (4000 rpm, one hour). The reduction of $AgNO_3$ with *M. communis* leaf extract was confirmed by dark brown color alteration of the solution[24]. After determining the average AgNPs crystal size, the FE-SEM (Model XL30, Philips, Eindhoven) was applied to assess the morphology, and the elemental analysis of AgNPs and the FT-IR analysis was performed via spectrophotometer (Germany, Bruker, Model: ALPHA). The peak absorbance of AgNPs was obtained in the range of 300 to 600 nm via an UV-visible spectrophotometer (Tomas, UV 331). The TEM technique revealed the average diameter size of 91.68 nm.

In-vivo method to study AgNPs effects

Animals

Adult male rats from Wistar race (240 – 270 g, 6-7 weeks of age) were housed in 12h light/dark cycle in a standard room (21 ± 2◦C). Food and water consumption was ad libitum. The total number of animals was seventy, and ten rats in each group were randomly selected according to the previous published data [25]. Tehran University of Medical Sciences Ethics Committee (IR.TUMS.VCR.REC.1396.4033) approved completely experimental protocols.

Stereotaxic surgery

Anesthesia agents were Ketamine hydrochloride (65 mg/kg, i.p.) and xylazine (15 mg/kg, i.p.). The lateral ventricles were cannulated by a guide cannula (22G) during the stereotaxic surgery (-0.8 mm, 1.5 mm laterality, and 4 mm beneath the brain surface) [26]. A heating pad was used during surgery. The 0.5 mg/kg ketoprofen was injected after surgery to reduce pain and distress. The recovery periods were seven days. Then, an intra-ICV injections were performed by a Hamilton syringe. The ICV-route ensures that a similar dose of AgNPs reaches to the brain of all animals irrespective of variations in drug transport or elimination routes.

Treatment Procedures

The AgNPs (0.1, 1, 10, and 100 ppm) were prepared in the normal saline. The solution was dispersed with an ultrasonic shaker prior each administration. The volume of intra-ICV injections was similar in all animals. Animals were dedicated to 7 groups (10 rats in each group) accidentally: 1) Intact group: remained intact during the experiments; 2) Sham group received normal saline (0.9 %, intra-ICV); 3) Extract group received an intra-ICV injection of leaf extract; 4) In the AgNPs groups, different doses of green-synthesized AgNPs (0.1, 1, 10 and 100 ppm, intra-ICV) were injected.

The open field

Motor activity of all rats was evaluated one week after surgery by the open field test. Three parameters of the number of line cross, frequency of rearing and grooming were recorded as described previously[27].

Y-maze

Alternation behavior was assessed 13 days after saline, extract or AgNPs administration for 8 minutes duration. A digital camera was used for recording the sequence of entries into the arms. The olfactory cues in the Y maze apparatus removed by alcohol swab before each test.

Novel object recognition (NOR)

The test based on the animal's desire to explore the new objects. The rats were allowed to navigate in the chamber for 10 minutes while two similar objects at a distance from each other placed in the chamber. After an hour, the new object was substitute with one of the old objects. The exploration time in the chamber was three minutes. The exploring time for new and old objects were recorded by a camera. The box and objects were cleaned in order to abolish the olfactory cues. Recognition index scores were calculated as the percentage of exploration time of novel object divided by total exploration time of new plus familiar object [28].

Elevated plus maze (EPM)

The EPM device had two closed and two open arms (50×10 cm) located in the opposite direction. The height was 50 cm above the floor and rats allowed to search freely for 5 min. The recorded films were used for calculation of the open arms time (OAT %), and the entrance to open arms (OAE %) in percentage as explained before[29].

Passive avoidance memory

The shuttle box apparatus was used for the measurement of passive avoidance memory. As mentioned before [29], the delay time of entry into the dark side of the box was recorded as step-through latency (STL). The time that animals spent in the dark chamber was reported as TDC.

Hippocampal MDA and SOD measurements

At the end of experiments, after animal decapitation, the hippocampus tissues were extracted and homogenized. The supernatants of homogenates kept at -70°C. The total protein concentrations were evaluated via the Bradford technique [30]. Lipid peroxidation level and SOD activity were determined based on the kit instructions.

Lipophilic fluorescent products (LFPs) assay

The extraction of hippocampus LFPs were based on the Goldstein and McDonagh description [31], and Wilhelm and Herget's modification [31]. The cold PBS (1:10 w/v) was used for hippocampus homogenization. The one ml of hippocampus homogenates was mixed with four ml of chloroform and methanol (2:1, v/v). After shaking and adding the distilled water and centrifuge (200×g, 20 min), the lower phase was used for fluorescent assay [32, 33]. To identify fluorescence maxima, all samples were analyzed and the fluorescence was measured in two synchronous fluorescence spectra, 25, and 50 nm difference between excitation and emission according to the previous our study [25].

Statistical analysis

The statistical analysis software was GraphPad Prism (version 7.04). After the normality evaluation by the Shapiro-Wilk test, the locomotion data, behavioral tasks, MDA level, and SOD activity were compared using one-way analysis of variance (ANOVA). The Tukey's test was considered as the post hoc. The two-way analysis of variance and repeated measure were performed for the fluorescence intensity comparisons. Findings were reported as the mean ± SEM. The exact p-value was provided for all variables.

RESULTS

3.1. Physicochemical properties of green-synthetized AgNPs

Spectroscopy of UV-visible: The AgNPs excitation absorption was around 320-370 nm and absorption peak intensity was 1.53 a.u (Fig.1A).

TEM and Zeta potential: The average diameter size of 91.68 nm was detected by TEM images (Fig.1B). There were different shapes involving spherical, triangular, and hexagonal. In addition, zeta potential was -17.4 mV (Fig.1C). The zeta potential was comparable to other studies about the AgNPs green synthesis [33, 34]. The Coulombic repulsion forces due to the negative surface potentials of AgNPs prevent aggregation.

X-ray diffraction analysis (XRD) and Fourier-transform infrared spectroscopy (FTIR): The

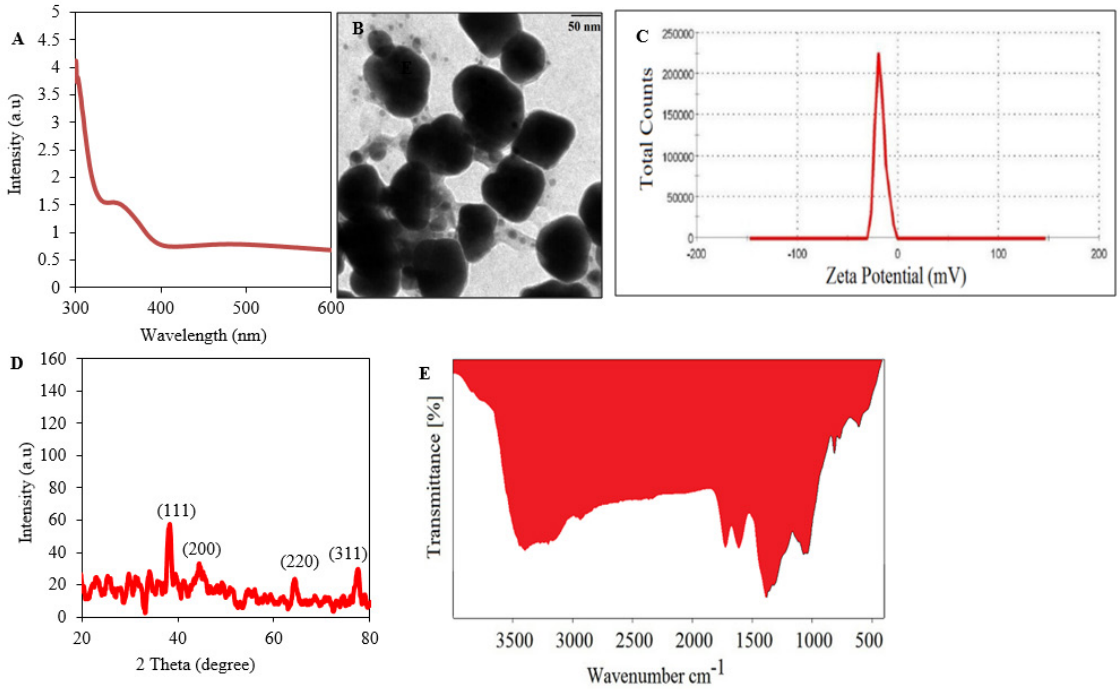

Fig. 1. Characteristics of green-synthetized AgNPs
A) UV-Visible spectra of synthesized AgNPs by aqueous leaf extracts of M. communis B) TEM images of AgNPs. C) Zeta potential results of AgNPs. D) The X-ray diffraction study and E) Spectroscopy of Fourier-transform infrared

Table1. Alteration of locomotor activity, rearing and grooming behaviors in the open field test. Animals received the ICV-injection of saline, extract or AgNPs (0.1, 1, 10, and 100 ppm). The body weight were recorded before and after the experiment. There was no significant difference among groups. Data are expressed as mean ± SEM (n=10).

	Open field			Body Weight	
Groups	**Locomotion**	**Rearing**	**Grooming**	**Before**	**After**
Intact	179.9± 5.7	5.3± 0.5	4.1± 0.4	243.7± 3.0	275.2± 2.0
Sham	178.7± 6.0	4.4± 0.7	3.9± 0.6	246.0± 1.9	274.9± 2.8
Extract	148.3± 9.9	4.2± 0.9	4.3± 0.6	245.0± 2.7	271.7± 1.6
AgNPs (0.1 ppm)	154.8± 10.5	4.8± 0.7	4.5± 0.5	248.7± 3.7	277.0± 2.3
AgNPs (1 ppm)	170.2± 12.3	4.3± 0.5	4.5± 0.5	250.9± 3.1	272.3± 2.2
AgNPs (10 ppm)	158.5± 11.4	4.5± 0.2	2.8± 0.8	246.9± 2.8	278.3± 2.2
AgNPs (100 ppm)	180.3± 12.8	4.0± 0.3	4.6± 0.4	250.5± 3.0	279.7± 1.9

XRD technique was used to assess crystal structure and AgNPs phase purity. The AgNPs diffraction peaks has been shown in Fig.1D. The AgNPs demonstrated 2 theta degrees of 38.22°, 44.27°, 63.96°, and 77.21° (111), (200), (220), and (311) indices respectively (JCPDS card no: 65-2871). In addition, crystal sizes 72 nm. The FTIR analysis showed several functional groups, including amine, carboxylic acid, ketone, aldehyde, phenol, and sulfoxide. There were prominent peaks, including 3397.85, 1723.53, 1612.53, 1386.27, 1070.29 cm^{-1} for N-H, C=O, and C=O stretching, as well as C-H bending, and S=O.

AgNPs Effects on behavioral indices

The locomotion ($F(6,63)=1.69$, $p=0.13$), rearing numbers ($F(6, 63)=1.30$, $p=0.26$), and grooming behavior ($F(6, 63)=1.01$, $p=0.42$) were alike in different groups (Table 1). The weight of animals was recorded two times, at the beginning

and research end. The body weight gain among groups before ($F(6, 63)=0.85$, $p=0.53$) and after ($F(6, 63)=1.77$, $p=0.11$, Table 1) experiments were similar.

Working memory in the Y-maze

We observed no significant difference regarding the alternative behavior among intact, sham and extract groups ($F(6, 63)=6.44$, $p=0.98$, Fig.2A). The same statistical results were found for 0.1 ppm (64.8 ± 3.6, vs. 67.3±2.87, $p=0.99$), and one ppm (60 ± 2.53, $p=0.34$) of AgNPs compared with the sham group. The percent of alternative behavior significantly decreased in groups that received 10 (55.6 ± 1.36, $p=0.017$) and 100 (53.2 ± 2.13, $p=0.002$) ppm AgNPs. The number of total arm entries were similar among groups ($F(6,63)=0.64$, $p=0.69$, Fig.2B).

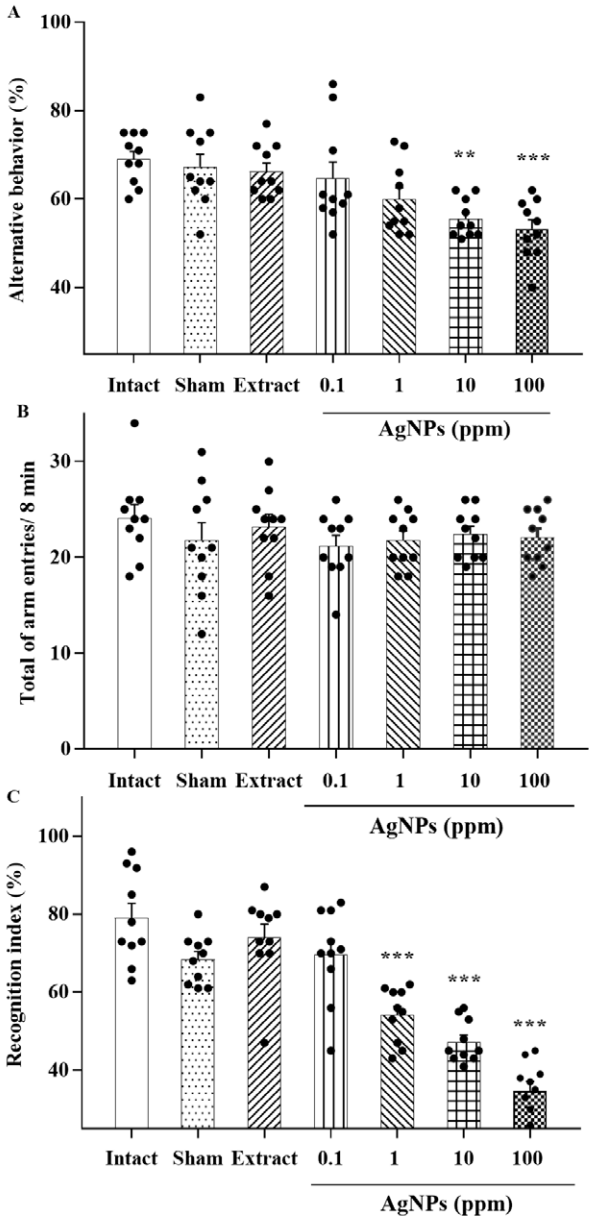

Fig. 2. Alterations in behavioral indices in the Y maze and object recognition tests
A) The percentage of spontaneous alternation, and B) The number of arm entries in the Y-maze test. C) The recognition index in the NOR test. Findings are shown as mean ± SEM (n=10).

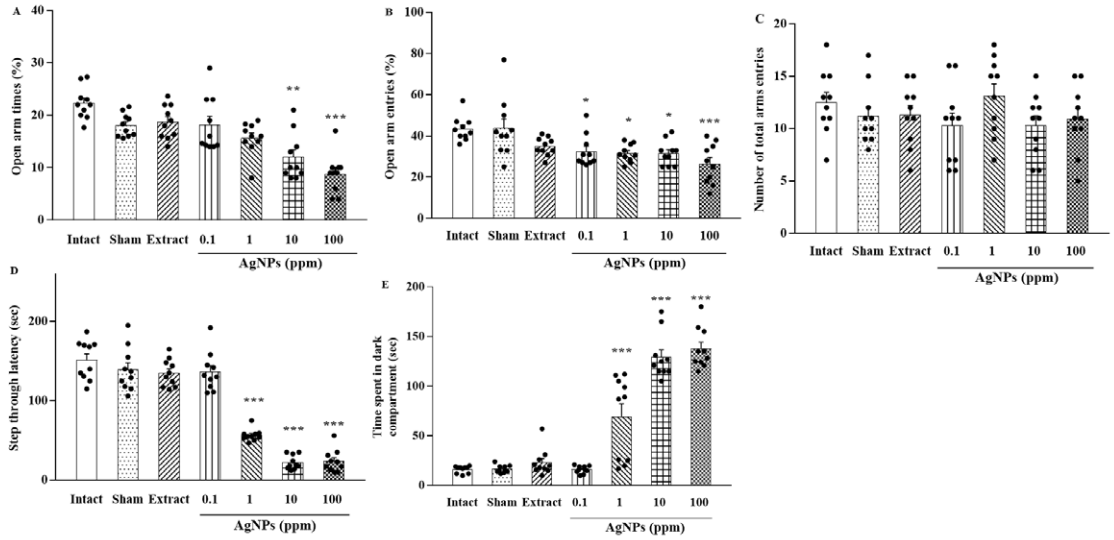

Fig. 3. Alterations in behavioral indices in the EPM and shuttle box tests

A) Time spent in the open arms in percentage, B) The open arm entries in percentage, C) The total number of arm entries, D) Alterations of step-through latency (STL), and E) Time spent in dark component (TDC) in the shuttle box test. Data are presented as mean ± SEM (n=10).

Recognition memory in the NOR test

Recognition index was significantly altered (F(6, 63)=31.42, p=0.000, Fig.2C). We found no significant difference among intact (79.08±3.7), sham (68.4±2.007), and extract (74 ±3.46) groups. The same condition was detected between 0.1 ppm (69.6 ± 3.73, p=0.99) and the sham group. However, the one (54.2 ±2.21, p=0.014), 10 (47.3±1.71, p<0.0001) and 100 (34.7 ±2.45, p<0.0001) ppm of AgNPs caused significant reduction in recognition index when matched with the sham group data.

Anxiety–like behavior in the EPM test

The OAT% (F (6, 63)=15.0, p=0.000) and OAE% (F (6, 63)=6.14, p=0.000) were significantly changed. The alterations of OAT% (22.3 ±0.97 vs. 18.1 ± 0.7, p=0.16, Fig.3A) and OAE% (43.4±1.88 vs. 43.8 ± 4.57, p=0.99, Fig.3B) were similar in the intact and sham groups. The same result was detected between the intact and extract groups in OAT% (18.7 ±1.02, p=0.32) and OAE% (35.0 ± 1.39, p=0.26). AgNPs administration, 0.1 (18.1±1.65, p=0.99), and 1ppm (15.6±0.98, p=0.75) had no significant effects on OAT% versus the sham group. However, the 0.1 (32.6±2.47, p=0.048) and 1ppm (31.6±1.37, p=0.02) caused a significant reduction in OAE%. The 10 and 100 ppm significantly decreased OAT% (12±1.41, p=0.008; 8.8±1.18, p=0.001) and OAE% (31.6±1.89, p=0.02; 26.5±3.11, p=0.0001) as compared to the sham group. The changes in the number of total arm entries among groups (F (6,63)=1.11, p=0.36, Fig.3C) were not significant. These results imply that, the doses of 10 and 100 ppm were anxiogenic.

Passive avoidance memory test

We observed the significant changes in the STL (F(6, 63)=90.0, p=0.000), and TDC (F(6, 63)=73.24, p=0.000). The differences between the intact and sham groups in the STL (151±7.84 vs.139±8.75, p=0.79, Fig.3D) and TDC (16.2±1.1 vs.16.5±1.2, p=0.99, Fig.3E) were nonsignificant. The STL (135±5.52, p=0.47) and TDC (23.1±4.19, p=0.98) were similar in the intact and extract groups. The AgNPs (0.1 ppm) had no significant effects on STL (137±7.81, p=0.99) and TDC (16.1±1.17, p=0.99) versus the sham group. While, the one (56.4±2.38, p<0.0001), 10 (22.3±2.82), and 100 (23.6±4.48, p<0.0001) ppm caused a significant reduction in the STL and TDC (69.1±13.9; 129.4±7.19; 137.7±6.49) versus the sham group.

Hippocampal MDA levels and SOD activity

We observed a significant alteration in MDA level among groups (F(6,63)=147.2, p=0.000, µmol/mg protein, Fig.4A). The intact and sham groups displayed no significant difference (3.01±0.31 vs. 3.22±0.52, p=0.99). The extract showed no significant changes versus the sham groups (4.86±0.71, p=0.71). We detected no significant

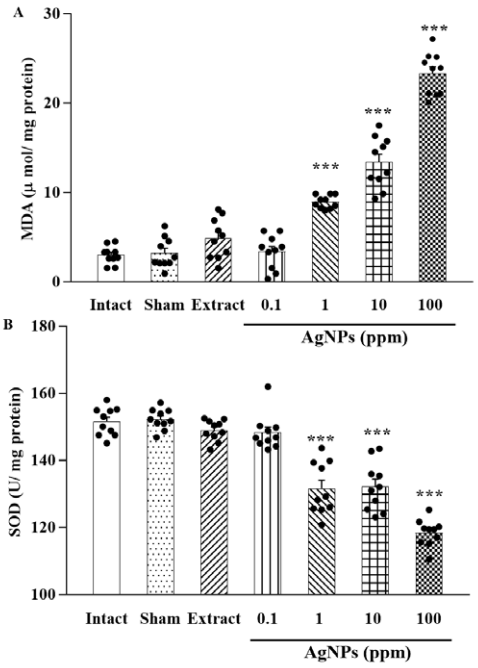

Fig. 4. Alterations of MDA and SOD activity in the hippocampus
(A) The doses of 1, 10, 100 ppm of AgNPs significantly increased the MDA levels and (B) decreased the SOD activity. Columns are mean ± SEM of data (n=10).

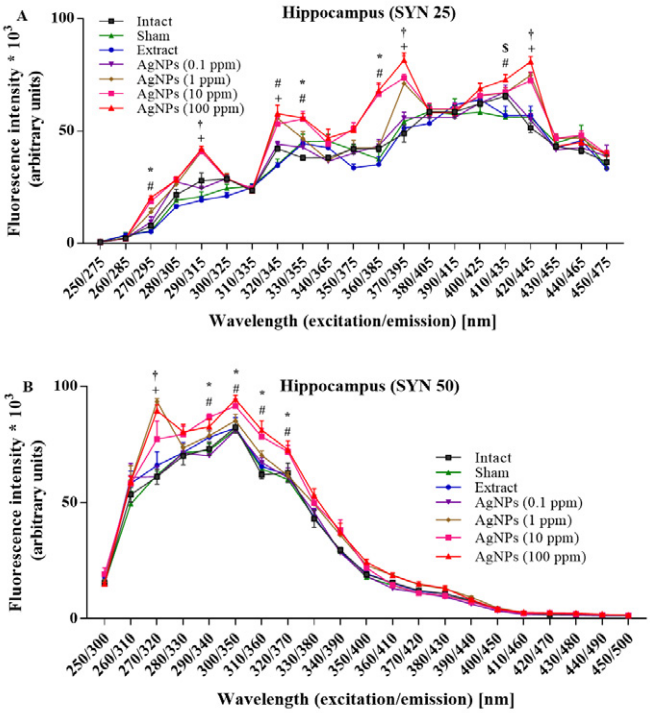

Fig. 5. Effect of AgNPs administration on LFPs spectra
The hippocampal synchronous fluorescence spectra of LFPs in SYN25 (A) and SYN50 (B). The fluorescence intensity was expressed in arbitrary units (*10^3). The points are mean ± SEM. *, specifies the significancy ($p<0.05$) between sham and 10 and 100 ppm groups. +, shows the significant change between sham and 1, 10, and 100 ppm groups ($p<0.05$). ≠, determines a significant alteration between AgNPs-0.1 and AgNPs-100 ppm groups ($p<0.05$). †, designates significancy between 0.1 ppm and 1, 10, 100 ppm groups ($p<0.05$). $, displays $p<0.05$ between sham and all AgNPs groups (n=10 in each group).

difference between the AgNPs (0.1 ppm) and the sham group (3.38±0.59, p=0.99). The AgNPs of 1(8.97±0.23), 10 (13.4±0.89) and 100 (23.3±0.74) ppm caused a significant rise in MDA level when checked with the sham group.

Our finding revealed the significant change in SOD activity (F(6,63)=65.27, P=0.000, U/mg protein, Fig.4B). The result of comparison between the intact and sham groups were 152±1.34 vs. 152±0.97, p=0.99. The same results were observed about the SOD activity in the extract (149±0.99, p=0.33) and 0.1 ppm AgNPs group (148±1.69, p=0.56) compared with the sham group. The SOD activity was decreased in one (132±2.48), 10 (132±2.3) and 100 (118±1.28) ppm AgNPs groups. Finally, the 0.1 ppm caused no oxidative induction.

AgNPs Effects on fluorescence spectra of LFPs in the hippocampus

A significant difference was detected between the fluorescence intensity ($F(20, 120)=537.9$, $p< 0.001$), and different groups ($F(6, 36) = 44.62$, $p<0.001$) and a significant interaction ($F(120, 720) = 4.97$, $p< 0.001$) was detected between them. In synchronous spectra analysis of the hippocampus, we found no significant difference between the intact, sham and extract groups in both synchrony of 25 and 50 nm. In SYN25, eight significant specific fluorescence maxima 270/295, 290/315, 320/ 345, 330/355, 360/385, 370/395, 410/435, and 420/445nm were detected in the 1, 10, and 100ppm AgNPs groups as matched with the sham data (Fig 5A). In SYN50, the most pronounced difference was observed at 270/320, 290/340, 300/350, 310/360 and 320/370 nm (Fig 5B).

DISCUSSION

Our finding revealed the ICV-administration of green-synthesized AgNPs (10, and 100 ppm) caused memory impairment and induced anxiety-like behavior. In addition, seven significant fluorescence maxima were distinguished in the AgNPs groups (1, 10, and 100ppm). However, the 0.1 ppm of AgNPs had no effects on MDA, SOD activity and LFPs. Exposure to the low doses of AgNPs, possibly through the hormesis effect, resisted the neurotoxicity. We focused on the dorsal hippocampus for the reason that, it is crucial for spatial learning[35] , retention of object recognition [36], and rat's passive avoidance memory [37].

The antioxidant and anti-inflammatory effects of AgNPs have been reported [8] and their usage has been dramatically enhanced. The green synthesis mediates biocompatible AgNPs for in vivo administration [38]. The plant extracts contribute to the stabilization of silver ions [39] and occupy the surface of nanoparticles [40], augmenting the potentiality of the nanoparticles [16]. Toxicity of chemical synthesized AgNPs to neurons, astrocytes and glial cells has been reported [41-43]. The neurotoxicity of various sized (25, 40, and 80 nm) silver nanoparticles have also been studied [44]. The larger AgNPs in comparison with the smaller particles, has less effects on rat brain microvessels to produce an inflammatory response. The ROS production and NMDA receptor activation have been reported as important mechanisms of AgNPs neurotoxicity in cultured neurons [45].

Nevertheless, the size, dose, and exposure time of AgNPs are important issues in biological responses. In the current study, the effects of AgNPs were dose-dependent. We found that 0.1 ppm caused no oxidative damage and cognitive impairment which may be due to the hormesis effect. We observed that high doses of AgNPs (10, and 100 ppm) induced working memory damage. The NOR task that depends on the integrity of the temporal regions [46], and is helpful for the cognitive deficit detection [47], was also impaired. In addition, the EPM results showed that high doses of AgNPs were anxiogenic.

Our data revealed the passive avoidance memory impairment in animals treated by high doses of AgNPs as indicated by a decrease in the STL and an increase in TDC. The high doses of AgNPs caused lipid peroxidation demonstrated by a rise in the hippocampal MDA level and was accompanied by a decrease in the activity of SOD. The nanoparticles neurotoxicity may be related to oxidative stress [48]. After AgNPs internalization, the silver ions release, and their reaction via several targets initiate the cytotoxicity[12] and induce oxidative stress.

We can interpret that cognitive impairment in the high doses of AgNPs groups was associated with an oxidative imbalance in the hippocampus tissue. High MDA level is a non-specific or common component in various diseases. We further evaluated the alteration of redox homeostasis by the measurement of fluorescence intensity of LFPs. The fluorescence intensity peaks were detected in specific excitation/emissions. The pattern of alterations was not the same in different doses implying the involvement of different LFPs

composition. Monitoring the patterns of changes in the fluorescent spectra of LFPs may help to find the most appropriate biomarker to evaluate nanoparticle toxicity.

In addition, the AgNPs antioxidant effects have been reported in other studies. For instance, Gonzalez-Carter, et al. showed their antioxidant effects against lipopolysaccharide-reactive oxygen species production[8]. Metallothioneins are antioxidants and interact with amyloidogenic peptides, and their up-regulation has been proposed as a therapeutic approach [49]. Interestingly, astrocytes exposure to AgNPs caused metallothioneins up-regulation [50]. Therefore, AgNPs may prevent oxidative damage by a compensatory mechanism such as metallothioneins' contribution. More studies are required to confirm these aspects. -

CONCLUSION

The ICV-AgNPs (10, and 100 ppm) administration caused memory impairment and altered the hippocampal redox status, verified by a rise in MDA level and decreased SOD activity. We further confirmed the alteration of redox status by detecting an elevated fluorescence intensity of LFPs in hippocampus. However, the low dose of AgNPs (0.1 ppm), possibly through the hormesis effect, had no destructive effects on behavioral indices and redox status. Understanding the biological effects of AgNPs can be used to make future safe classes of AgNPs in the food and drug industries.

ACKNOWLEDGMENTS

The Electrophysiology Research Center, Neuroscience Institute, Tehran University of Medical Sciences (Grant numbers: 96-03-139-36130) have supported this work, and we would like to thank them for their financial support of this research project.

DECLARATION OF COMPETING INTEREST

The authors declare that they have no conflict of interest.

ABBREVIATIONS

FTIR: Spectroscopy of Fourier-transform infrared, Green-synthesized, silver nanoparticles: AgNPs, ICV: Intracerebroventricular, LFPs: Lipophilic fluorescent products, MDA: malondialdehyde, SOD: superoxide dismutase, TEM: transmission electron microscopy

REFERENCES

1. Dąbrowska-Bouta B, Sulkowski G, Strużyński W, Strużyńska L. Prolonged exposure to silver nanoparticles results in oxidative stress in cerebral myelin. Neurotoxicity Research, 2019;35 (3):495-504. https://doi.org/10.1007/s12640-018-9977-0
2. Skalska J, Dąbrowska-Bouta B, Strużyńska L. Oxidative stress in rat brain but not in liver following oral administration of a low dose of nanoparticulate silver. Food and Chemical Toxicology, 2016;97:307-315. https://doi.org/10.1016/j.fct.2016.09.026
3. Tang J, Xiong L, Zhou G, Wang S, Wang J, Liu L, Li J, Yuan F, Lu S, Wan Z. Silver nanoparticles crossing through and distribution in the blood-brain barrier in vitro. Journal of nanoscience and nanotechnology, 2010;10 (10):6313-6317. https://doi.org/10.1166/jnn.2010.2625
4. Ziemińska E, Strużyńska L. Zinc modulates nanosilver-induced toxicity in primary neuronal cultures. Neurotoxicity Research, 2016;29 (2):325-343. https://doi.org/10.1007/s12640-015-9583-3
5. Lee JH, Kim YS, Song KS, Ryu HR, Sung JH, Park JD, Park HM, Song NW, Shin BS, Marshak D. Biopersistence of silver nanoparticles in tissues from Sprague-Dawley rats. Particle and fibre toxicology, 2013;10 (1):1-14. https://doi.org/10.1186/1743-8977-10-36
6. Antsiferova A, Kopaeva M, Kashkarov P. Effects of prolonged silver nanoparticle exposure on the contextual cognition and behavior of mammals. Materials, 2018;11 (4):558. https://doi.org/10.3390/ma11040558
7. Greish K, Alqahtani AA, Alotaibi AF, Abdulla AM, Bukelly AT, Alsobyani FM, Alharbi GH, Alkiyumi IS, Aldawish MM, Alshahrani TF. The effect of silver nanoparticles on learning, memory and social interaction in BALB/C mice. International journal of environmental research and public health, 2019;16 (1):148. https://doi.org/10.3390/ijerph16010148
8. Gonzalez-Carter DA, Leo BF, Ruenraroengsak P, Chen S, Goode AE, Theodorou IG, Chung KF, Carzaniga R, Shaffer MS, Dexter DT. Silver nanoparticles reduce brain inflammation and related neurotoxicity through induction of H2S-synthesizing enzymes. Scientific reports, 2017;7 (1):1-14. https://doi.org/10.1038/srep42871
9. Rosman NSR, Harun NA, Idris I, Ismail WIW. Eco-friendly silver nanoparticles (AgNPs) fabricated by green synthesis using the crude extract of marine polychaete, Marphysa moribidii: biosynthesis, characterisation, and antibacterial applications. Heliyon, 2020;6 (11):e05462.
10. Guo Z, Chen G, Zeng G, Huang Z, Chen A, Hu L, Wang J, Jiang L. Cysteine-induced hormesis effect of silver nanoparticles. Toxicology research, 2016;5 (5):1268-1272. https://doi.org/10.1039/C6TX00222F
11. Calabrese EJ. Preconditioning is hormesis part I: Documentation, dose-response features and mechanistic foundations. Pharmacological Research, 2016;110:242-264. https://doi.org/10.1016/j.phrs.2015.12.021
12. De Matteis V, Malvindi MA, Galeone A, Brunetti V, De Luca E, Kote S, Kshirsagar P, Sabella S, Bardi G, Pompa PP. Negligible particle-specific toxicity mechanism of silver nanoparticles: the role of Ag+ ion release in the cytosol. Nanomedicine: Nanotechnology, Biology and Medicine, 2015;11 (3):731-739.
https://doi.org/10.1016/j.nano.2014.11.002

13. Boudreau MD, Imam MS, Paredes AM, Bryant MS, Cunningham CK, Felton RP, Jones MY, Davis KJ, Olson GR. Differential effects of silver nanoparticles and silver ions on tissue accumulation, distribution, and toxicity in the Sprague Dawley rat following daily oral gavage administration for 13 weeks. Toxicological Sciences, 2016;150 (1):131-160. https://doi.org/10.1093/toxsci/kfv318
14. Chahardoli A, Karimi N, Fattahi A. Biosynthesis, characterization, antimicrobial and cytotoxic effects of silver nanoparticles using Nigella arvensis seed extract. Iranian journal of pharmaceutical research: IJPR, 2017;16 (3):1167. https://dx.doi.org/10.22037/ijpr.2017.2066
15. Gardeli C, Vassiliki P, Athanasios M, Kibouris T, Komaitis M. Essential oil composition of Pistacia lentiscus L. and Myrtus communis L.: Evaluation of antioxidant capacity of methanolic extracts. Food chemistry, 2008;107 (3):1120-1130. https://doi.org/10.1016/j.foodchem.2007.09.036
16. Gour A, Jain NK. Advances in green synthesis of nanoparticles. Artificial cells, nanomedicine, and biotechnology, 2019;47 (1):844-851. https://doi.org/10.1080/21691401.2019.1577878
17. Hajiaghaee R, Faizi M, Shahmohammadi Z, Abdollahnejad F, Naghdibadi H, Najafi F, Razmi A. Hydroalcoholic extract of Myrtus communis can alter anxiety and sleep parameters: a behavioural and EEG sleep pattern study in mice and rats. Pharmaceutical biology, 2016;54 (10):2141-2148. https://doi.org/10.3109/13880209.2016.1148175
18. Messaoud C, Boussaid M. Myrtus communis berry color morphs: A comparative analysis of essential oils, fatty acids, phenolic compounds, and antioxidant activities. Chemistry & biodiversity, 2011;8 (2):300-310. https://doi.org/10.1002/cbdv.201000088
19. Hayder N, Bouhlel I, Skandrani I, Kadri M, Steiman R, Guiraud P, Mariotte A-M, Ghedira K, Dijoux-Franca M-G, Chekir-Ghedira L. In vitro antioxidant and antigenotoxic potentials of myricetin-3-o-galactoside and myricetin-3-o-rhamnoside from Myrtus communis: Modulation of expression of genes involved in cell defence system using cDNA microarray. Toxicology in vitro, 2008;22 (3):567-581. https://doi.org/10.1016/j.tiv.2007.11.015
20. Ivica J, Wilhelm J. Lipophilic fluorescent products of free radicals. Biomedical Papers of the Medical Faculty of Palacky University in Olomouc, 2014;158 (3).
21. Chio K, Reiss U, Fletcher B, Tappel A. Peroxidation of subcellular organelles: formation of lipofuscinlike fluorescent pigments. Science, 1969;166 (3912):1535-1536. https://doi.org/10.1126/science.166.3912.1535
22. Frankel E. Lipid Oxidation. Dundee. Scotland: The Oily Press LTD, 1998.
23. Alavi M, Karimi N. Characterization, antibacterial, total antioxidant, scavenging, reducing power and ion chelating activities of green synthesized silver, copper and titanium dioxide nanoparticles using Artemisia haussknechtii leaf extract. Artificial cells, nanomedicine, and biotechnology, 2018;46 (8):2066-2081. https://doi.org/10.1080/21691401.2017.1408121
24. Alavi M, Karimi N, Valadbeigi T. Antibacterial, antibiofilm, antiquorum sensing, antimotility, and antioxidant activities of green fabricated Ag, Cu, TiO2, ZnO, and Fe3O4 NPs via protoparmeliopsis muralis lichen aqueous extract against multi-drug-resistant bacteria. ACS Biomaterials Science & Engineering, 2019;5 (9):4228-4243. https://doi.org/10.1021/acsbiomaterials.9b00274
25. Tarbali S, Zahmatkesh M, Torkaman-Boutorabi A, Khodagholi F. Assessment of lipophilic fluorescence products in β-amyloid-induced cognitive decline: A parallel track in hippocampus, CSF, plasma and erythrocytes. Experimental gerontology, 2022;157:111645. https://doi.org/10.1016/j.exger.2021.111645
26. Paxinos G, Watson C. The rat brain in stereotaxic coordinates: hard cover edition: Elsevier; 2006.
27. Dezfouli MA, Zahmatkesh M, Farahmandfar M, Khodagholi F. Melatonin protective effect against amyloid β-induced neurotoxicity mediated by mitochondrial biogenesis; involvement of hippocampal Sirtuin-1 signaling pathway. Physiology & behavior, 2019;204:65-75. https://doi.org/10.1016/j.physbeh.2019.02.016
28. Marbouti L, Zahmatkesh M, Riahi E, Sadr SS. Inhibition of brain 17β-estradiol synthesis by letrozole induces cognitive decline in male and female rats. Neurobiology of Learning and Memory, 2020;175:107300. https://doi.org/10.1016/j.nlm.2020.107300
29. Aminyavari S, Zahmatkesh M, Khodagholi F, Sanati M. Anxiolytic impact of Apelin-13 in a rat model of Alzheimer's disease: Involvement of glucocorticoid receptor and FKBP5. Peptides, 2019;118:170102. https://doi.org/10.1016/j.peptides.2019.170102
30. Bradford MM. A rapid and sensitive method for the quantitation of microgram quantities of protein utilizing the principle of protein-dye binding. Analytical biochemistry, 1976;72 (1-2):248-254. https://doi.org/10.1006/abio.1976.9999
31. Goldstein B, McDonagh EM. Spectrofluorescent detection of in vivo red cell lipid peroxidation in patients treated with diaminodiphenylsulfone. The Journal of Clinical Investigation, 1976;57 (5):1302-1307. https://doi.org/10.1172/JCI108398
32. Patková J, Vojtíšek M, Tůma J, Vožeh F, Knotková J, Šantorová P, Wilhelm J. Evaluation of lipofuscin-like pigments as an index of lead-induced oxidative damage in the brain. Experimental and toxicologic pathology, 2012;64 (1-2):51-56. https://doi.org/10.1016/j.etp.2010.06.005
33. Skoumalova A, Ivica J, Šantorová P, Topinkova E, Wilhelm J. The lipid peroxidation products as possible markers of Alzheimer's disease in blood. Experimental Gerontology, 2011;46 (1):38-42. https://doi.org/10.1016/j.exger.2010.09.015
34. Jyoti K, Singh A. Green synthesis of nanostructured silver particles and their catalytic application in dye degradation. J Genet Eng Biotechnol, 2016;14 (2):311-317. https://doi.org/10.1016/j.jgeb.2016.09.005
35. Moser MB, Moser EI, Forrest E, Andersen P, Morris RG. Spatial learning with a minislab in the dorsal hippocampus. Proc Natl Acad Sci U S A, 1995;92 (21):9697-9701. https://doi.org/10.1073/pnas.92.21.9697
36. Cohen SJ, Stackman RW, Jr. Assessing rodent hippocampal involvement in the novel object recognition task. A review. Behav Brain Res, 2015;285:105-117. https://doi.org/10.1016/j.bbr.2014.08.002
37. Lorenzini CA, Baldi E, Bucherelli C, Sacchetti B, Tassoni G. Role of dorsal hippocampus in acquisition, consolidation and retrieval of rat's passive avoidance response: a tetrodotoxin functional inactivation study. Brain Res, 1996;730 (1-2):32-39. https://doi.org/10.1016/0006-8993(96)00427-1
38. Singh P, Kim YJ, Wang C, Mathiyalagan R, Yang DC. The

development of a green approach for the biosynthesis of silver and gold nanoparticles by using Panax ginseng root extract, and their biological applications. Artif Cells Nanomed Biotechnol, 2016;44 (4):1150-1157.
https://doi.org/10.3109/21691401.2015.1011809

39. Khatoon N, Mazumder J, Sardar M. Biotechnological Applications of Green Synthesized Silver Nanoparticles. Journal of Nanosciences: Current Research, 2017;2:1-8. https://doi.org/10.4172/2572-0813.1000107
40. Bélteky P, Rónavári A, Igaz N, Szerencsés B, Tóth IY, Pfeiffer I, Kiricsi M, Kónya Z. Silver nanoparticles: aggregation behavior in biorelevant conditions and its impact on biological activity. Int J Nanomedicine, 2019;14:667-687. https://doi.org/10.2147/IJN.S185965
41. Haase A, Rott S, Mantion A, Graf P, Plendl J, Thünemann AF, Meier WP, Taubert A, Luch A, Reiser G. Effects of silver nanoparticles on primary mixed neural cell cultures: uptake, oxidative stress and acute calcium responses. Toxicol Sci, 2012;126 (2):457-468. https://doi.org/10.1093/toxsci/kfs003
42. Hsiao IL, Hsieh YK, Chuang CY, Wang CF, Huang YJ. Effects of silver nanoparticles on the interactions of neuron- and glia-like cells: Toxicity, uptake mechanisms, and lysosomal tracking. Environ Toxicol, 2017;32 (6):1742-1753. https://doi.org/10.1002/tox.22397
43. Pani J, Singh R, Sankarsan P, Rajeev S. The Review of Small Size Silver Nanoparticle Neurotoxicity: A Repeat Study. Omic group journal of cytology and histology, 2017;8:2157-7099(2151.
44. Trickler WJ, Lantz SM, Murdock RC, Schrand AM, Robinson BL, Newport GD, Schlager JJ, Oldenburg SJ, Paule MG, Slikker W, Jr., Hussain SM, Ali SF. Silver nanoparticle induced blood-brain barrier inflammation and increased permeability in primary rat brain microvessel endothelial cells. Toxicol Sci, 2010;118 (1):160-170. https://doi.org/10.1093/toxsci/kfq244
45. Ziemińska E, Stafiej A, Strużyńska L. The role of the glutamatergic NMDA receptor in nanosilver-evoked neurotoxicity in primary cultures of cerebellar granule cells. Toxicology, 2014;315:38-48. https://doi.org/10.1016/j.tox.2013.11.008
46. Whitwell JL, Przybelski SA, Weigand SD, Knopman DS, Boeve BF, Petersen RC, Jack CR, Jr. 3D maps from multiple MRI illustrate changing atrophy patterns as subjects progress from mild cognitive impairment to Alzheimer's disease. Brain, 2007;130 (Pt 7):1777-1786.
47. Grayson B, Leger M, Piercy C, Adamson L, Harte M, Neill JC. Assessment of disease-related cognitive impairments using the novel object recognition (NOR) task in rodents. Behav Brain Res, 2015;285:176-193. https://doi.org/10.1016/j.bbr.2014.10.025
48. Song B, Zhang Y, Liu J, Feng X, Zhou T, Shao L. Is Neurotoxicity of Metallic Nanoparticles the Cascades of Oxidative Stress? Nanoscale Res Lett, 2016;11 (1):291. https://doi.org/10.1186/s11671-016-1508-4
49. Atrián-Blasco E, Santoro A, Pountney DL, Meloni G, Hureau C, Faller P. Chemistry of mammalian metallothioneins and their interaction with amyloidogenic peptides and proteins. Chem Soc Rev, 2017;46 (24):7683-7693. https://doi.org/10.1039/C7CS00448F
50. Luther EM, Schmidt MM, Diendorf J, Epple M, Dringen R. Upregulation of metallothioneins after exposure of cultured primary astrocytes to silver nanoparticles. Neurochem Res, 2012;37 (8):1639-1648. https://doi.org/10.1007/s11064-012-0767-4